Animal Nutrition 10 (2022) 216–222

Contents lists available at ScienceDirect

Animal Nutrition

journal homepage: http://www.keaipublishing.com/en/journals/aninu/

Short Communication

Localization of urea transporter B in the developing bovine rumen

Chongliang Zhong [a], Tamsin Lyons [a], Orla Heussaff [a], Evelyn Doyle [a], Eoin O'Hara [b, c], Sinead M. Waters [b], David Kenny [b], Gavin S. Stewart [a, *]

[a] School of Biology and Environmental Science, University College Dublin, Belfield, Dublin 4, Ireland
[b] Animal and Bioscience Research Department, Animal and Grassland Research and Innovation Centre, Teagasc, Grange, County Meath, Ireland
[c] Department of Agriculture, Food, and Nutritional Sciences, University of Alberta, Edmonton, Alberta, Canada

ARTICLE INFO

Article history:
Received 1 May 2021
Received in revised form
2 March 2022
Accepted 29 March 2022
Available online 28 April 2022

Keywords:
UT-B
Immunolocalization
Rumen
Bovine
Development

ABSTRACT

Urea nitrogen secreted from blood to rumen is a crucial factor shaping the symbiotic relationship between host ruminants and their microbial populations. Passage of urea across rumen epithelia is facilitated by urea transporter B (UT-B), but the long-term regulation of these proteins remains unclear. As ruminal function develops over a period of months, the developing rumen is an excellent model with which to investigate this regulation. Using rumen epithelium samples of calves from birth to 96 d of age, this study performed immunolocalization studies to localize and semi-quantify UT-B protein development. As expected, preliminary experiments confirmed that ruminal monocarboxylate transporter 1 (MCT1) short chain fatty acid transporter protein abundance increased with age ($P < 0.01$, $n = 4$). Further investigation revealed that ruminal UT-B was present in the first few weeks of life and initially detected in the basolateral membrane of stratum basale cells. Over the next 2 months, UT-B staining spread to other epithelial layers and semi-quantification indicated that UT-B abundance significantly increased with age ($P < 0.01$, $n = 4$ or 6). These changes were in line with the development of rumen function after the advent of solid feed intake and weaning, exhibiting a similar pattern to both MCT1 transporters and papillae growth. This study therefore confirmed age-dependent changes of in situ ruminal UT-B protein, adding to our understanding of the long-term regulation of ruminal urea transporters.

1. Introduction

The rumen ecosystem represents a classic example of a symbiotic relationship between host animals and microbial populations (Moraïs and Mizrahi, 2019). Since animals and commensal gut microbes are constantly exposed to limited nitrogen resources, nitrogen in the gastrointestinal tract is a crucial factor shaping this relationship (Reese et al., 2018) and is a fundamental driver of host–microbiome interactions (Holmes et al., 2017). Mechanisms have evolved in this low nitrogen setting to conserve nitrogen and maintain the symbiotic relationship with microbes. One important example is the urea nitrogen salvaging (UNS) process, through which ruminants can shift urea excretion from kidney to rumen (40% to 80% of synthesised urea) and where ureolytic bacteria adhering to the rumen wall can break urea down into ammonia (Stewart and Smith, 2005). This ammonia is used as a nitrogen resource for synthesis of microbial proteins, which provide a substantial metabolizable protein supply to the ruminant host (Stewart and Smith, 2005).

It has long been established that the entry of urea into the rumen is facilitated by urea transporter B2 (UT-B2) (Stewart et al., 2005; Coyle et al., 2016; Zhong et al., 2020). Unlike renal UT-A-mediated urea transport, UT-B2-mediated trans-cellular urea transport is constitutively activated and unaffected by known UT-A regulators, such as vasopressin (Tickle et al., 2009). Nevertheless, it remains unclear how the urea transport capacity of rumen epithelia is regulated through the UT-B2 proteins. Previous studies of the regulation of ruminal urea transporters have mainly focused on

* Corresponding author.
E-mail address: gavin.stewart@ucd.ie (G.S. Stewart).
Peer review under responsibility of Chinese Association of Animal Science and Veterinary Medicine.

Production and Hosting by Elsevier on behalf of KeAi

https://doi.org/10.1016/j.aninu.2022.03.006

manipulating diets of adult animals by altering dietary nitrogen levels. However, only weak associations have been found between urea flux across rumen and urea transporters under different dietary nitrogen levels (Marini and Van Amburgh, 2003; Marini et al., 2004; Ludden et al., 2009; Kristensen et al., 2010). Increasingly, studies have shown that UT-B transporters are more responsive to the changes of dietary energy levels and correlated with the resulting microbial short chain fatty acids (SCFA) (Simmons et al., 2009; Walpole et al., 2015). These results are in line with various ex vivo functional studies showing that urea transport capacity of rumen epithelium can be regulated by pH in the presence of SCFA and CO_2 (Abdoun et al., 2010; Lu et al., 2014). It has also been shown that SCFA and pH can regulate UT-B abundance in rumen-derived primary cells (Lu et al., 2015). These findings support the idea that urea plays a key physiological role in buffering microbially-derived SCFA in the rumen. In this process, ammonia produced from urea by bacterial urease can combine with H^+ ions to form ammonium ions, which can then be readily reabsorbed across the rumen epithelia (Stumpff, 2018).

Calves undergo a transition from pre-ruminant to ruminant, during which microbial colonization, fermentation capacity and need for UNS all increase (Stewart and Smith, 2005). The developing rumen is therefore an excellent in vivo model to observe the regulation of urea transporters. Indeed, Berends et al. quantified that the salvaged urea nitrogen contributes to 19% of nitrogen retention during the transition from pre-ruminants (milk fed calves) to ruminants (solid feed fed calves) (Berends et al., 2014). Importantly, in line with this, the *UT-B* mRNA expression also increased with solid feed intake (Berends et al., 2014). This again suggests microbial fermentation activity and derived production of SCFA might be the key long-term regulator of ruminal urea transporters. However, the protein localization and abundance of UT-B were not investigated. This current study therefore aimed to localize and semi-quantify in situ protein abundance of UT-B in the developing bovine rumen.

2. Materials and methods

2.1. Animals and tissue samples

All procedures were approved by the Teagasc Animal Ethics Committee and conducted under experimental license from the Irish Health Products Regulatory Authority, in accordance with the Cruelty to Animals Act 1876 and the European Communities (Amendments of the Cruelty to Animals Act, 1876) Regulations, 1994. The full details of this animal model using Aberdeen Angus heifers have been previously published (O'Hara et al., 2020). Briefly, before birth and irrespective of sex, calves were assigned to one of 6 groups and based on this they were euthanized at birth (D0, $n = 4$), at d 7 (D7, $n = 4$), 14 (D14, $n = 4$), 21 (D21, $n = 4$), 28 (D28, $n = 4$), or 96 (D96, $n = 6$) after birth. Calves not euthanized at birth could suckle their dams for 2 d post birth, at which point they were removed and penned individually. Calves were then reared on milk replacer (5 L/d, fed twice daily). From D7 onwards, calves had access to ad libitum concentrate. Calves were weaned at the age of 56 d (or earlier if consuming 1 kg concentrates per day for 3 consecutive days). After weaning, calves were offered 2 kg concentrate per day, with ad libitum water and hay, until they were euthanized at D96. Following euthanasia, samples of ventral sac rumen tissue were taken, washed in phosphate buffer solution, and fixed in 10% neutral buffered formalin. After fixation, samples were dehydrated with increasing concentrations of ethyl-alcohol (50% to 100%) using an automated processer (Tissue-TEK VIP, Sakura, Finetek) and embedded in paraffin wax.

2.2. Hematoxylin-eosin (H&E) staining and papillae measurements

The paraffin-embedded calf rumen tissues were cut into 4-μm sections using a microtome (Leitz RM2255) and mounted onto negatively charged glass slides. Samples were then stained with haematoxylin and eosin (H&E) using a Leica auto-stainer (Leica ST5020) and observed using a light microscope (Leica DM3000). Measurements of papillae length and width were taken at 50× magnification using a 1-cm graticule, with 10 well-orientated papillae measured per section. Tissue sections harvested from calves at birth (D0) had fewer papillae present, with only 4 available per section for measurement compared to the minimum of 10 measured per section from all other time points. Papilla length was measured from the tip to the base of the papilla (adjacent to the tunica muscularis layer). Papilla width was measured at the midpoint of the papilla, from the outside epithelial edges.

2.3. Immunohistochemistry and protein abundance score

Rumen papillae sections of 5 μm were cut and attached to slides (Thermo Scientific, Hungary). After overnight drying, sections were de-waxed in Neo-clear (Millipore, Germany), and rehydrated in a series of decreasing ethanol concentrations (100%, 90% and 70%). Sections were incubated in 0.3% (vol/vol) H_2O_2 in methanol at room temperature for 30 min and washed (3 × 10 min) in d 1 washing buffer containing 1% (wt/vol) bovine serum albumin (BSA), 0.2% (vol/vol) gelatine, 0.05% (wt/vol) saponin in phosphate buffered solution (PBS). They were incubated overnight at 4 °C in UT-B (1:250; hUTBc19) (Walpole et al., 2014) or monocarboxylate transporter 1 (MCT1) antibodies (1:2,000; AB1286-I, Millipore) diluted in a buffer containing 0.1% (wt/vol) BSA, 0.3% (vol/vol) Triton X-100 in PBS. Sections were then washed (3 × 10 min) in d 2 washing buffer containing 0.1% (wt/vol) BSA, 0.2% (vol/vol) gelatine, 0.05% (wt/vol) saponin in PBS, followed by incubation with a horseradish peroxidase-linked anti-rabbit secondary antibody at a dilution of 1:200 (for UT-B) or an anti-chicken antibody at 1:2,000 (for MCT1) for 1 h at room temperature. After further washes, sections were reacted with 3,3′-diaminobenzidine (Sigma-Aldrich, USA) for 10 min and counterstained with haematoxylin. After serial dehydration in ethanol (70%, 90% and 100%), stained sections were preserved using a mounting medium (Eukitt, Sigma-Aldrich, Germany) and coverslips. Negative controls were performed by replacing the primary antibody with its dilution buffer. For peptide competition analysis, UT-B primary antibody was pre-absorbed with its immunizing peptide (1 μg/μL) for 24 h or an equivalent amount of an irrelevant peptide.

Stained slides were examined under a light microscope (Leica, Germany) and representative staining was imaged, using a digital camera (DFC420C, Leica, Germany) with its software (Application Suit V4). To semi-quantitatively determine in situ protein abundance, signal strength was “blind” scored by 3 experienced examiners on a scale of 0 to 5, where 0 = none, 1 = very weak, 2 = weak, 3 = moderate, 4 = strong, and 5 = very strong. For each animal, the scores of the 3 examiners were averaged.

2.4. Statistical analysis

Data were visualized using ggplot2 package in R software environment. General linear models were used to test null hypotheses:

$$\text{Papillae length} = \beta_{\text{age}} + N\,(0,\ \sigma_i)\ ,$$

$$\log\,(\text{Papillae width}) = \beta_{\text{age}} + N\,(0,\ \sigma_i)\ ,$$

$$\text{UT-B expression score} = \beta_{\text{age}} + N\,(0,\ \sigma_i)\ ,$$

where β_{age} was the fitted effects of ages on the response, and $N\,(0, \sigma i)$ was the normally distributed error with zero mean and standard deviation σi. The models were fitted to the data by maximum likelihood using R statistical software. Residuals of these fitted models were consistent with model assumptions of normality, homogeneity of variance and independence. Once differences were

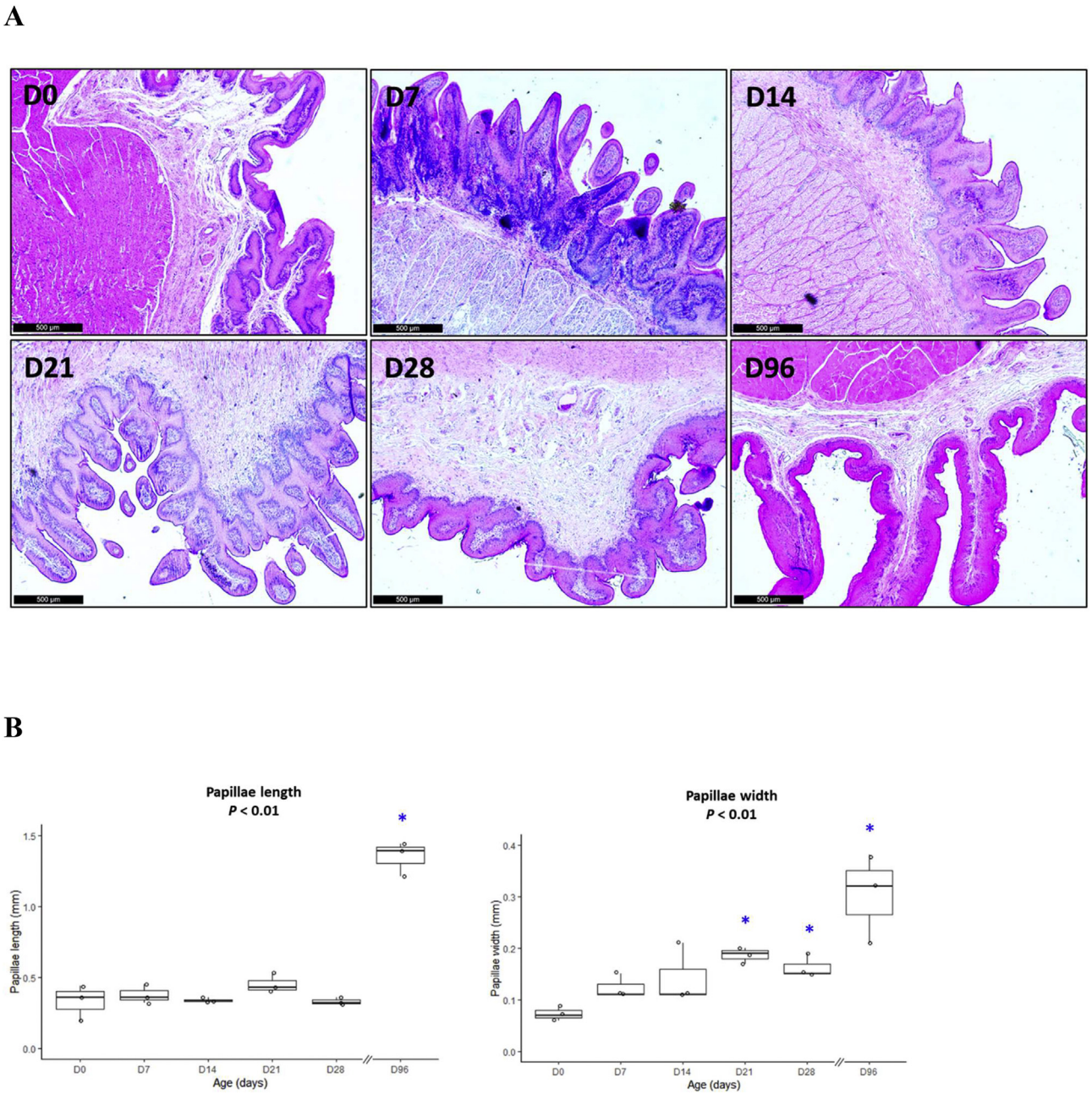

Fig. 1. Rumen papillae measurements at various ages. (A) Rumen tissues were taken from calves at birth (D0), and 7 (D7), 14 (D14), 21 (D21), 28 (D28) and 96 d of age (D96). Sections were stained with haematoxylin and eosin (H&E) and imaged under a light microscope at 50× magnification (showing 1 set of tissues). Scale bar = 500 μm. (B) Ten papillae of each animal were measured for length and width. Analysis of variance showed significant age dependent difference for papilla length ($P < 0.01$, $n = 3$) and width ($P < 0.01$, $n = 3$). D96 calves had 4-fold longer papillae than D0 (estimated means: 1.35 vs. 0.33 mm; $P < 0.01$), whereas the papilla length of D7, D14, D21, and D28 were not significantly different from that of D0 ($P > 0.05$, Tukey's HSD). The papillae width of D96 animals was 4-fold greater than that of D0 (estimated means: 0.29 vs. 0.07 mm; $P < 0.01$, Tukey's HSD). The papillae of D28 ($P < 0.05$) and D21 ($P < 0.01$) were also wider than that of D0, but those of D14 and D7 were not significantly different from D0 ($P > 0.05$, Tukey's HSD). The asterisk (*) indicates statistical difference ($P < 0.05$) from D0.

found, post hoc testing was performed using Tukey's HSD to test for differences between each pair of ages. When data transformation was made to meet model assumptions, original data were used to make box and dot plot, whereas *P*-value and estimated means were derived from transformed data (estimated means were back transformed). Hypothesis tests used a critical significance level of 5%.

3. Results

To examine the morphological development of calf rumen epithelia, sections were stained using a H&E method (Fig. 1A). Papillae length and width were both measured and found to differ with age (ANOVA, $P < 0.01$, $n = 3$; Fig. 1B). Papillae in the rumen of D96 calves (approximately 1,350 μm) were 4-fold longer than that of D0 calves (approximately 330 μm, $P < 0.01$, Tukey's HSD; Fig. 1B). In contrast, no differences of length were found among the ages of 0, 7, 14, 21, and 28 d ($P > 0.05$; Fig. 1B). Papillae width was greater in D21 (approximately 190 μm, $P < 0.01$, Tukey's test), D28 (approximately 160 μm, $P < 0.05$), and D96 (approximately 290 μm, $P < 0.01$) calves compared to D0 calves (approximately 70 μm; Fig. 1B).

For immunolocalization protocol validation, we first investigated the ruminal SCFA transporter MCT1, previously shown to increase with age at both mRNA and protein levels (Flaga et al., 2015). In the D0 animals, weak staining was dispersed in the cytoplasm throughout all epithelial cell layers (Fig. 2A). For D7 to D28 tissues, MCT1 signals were accumulated at the cell membrane of stratum basale cells, particularly the basolateral membrane (Fig. 2B, D28). For D96, strong cell membrane staining was detected throughout basale and spinosum layers (Fig. 2C). Statistical analysis confirmed a highly significant increase in "blind-scored" MCT1 staining as the rumen developed ($P < 0.01$, $n = 4$) (Fig. 2D).

Next, the cellular localization of UT-B protein was investigated and in D0 tissues only faint, cytoplasmic staining was observed (4 out of 4 animals) (Fig. 3A). For D7 to D28, positive immunostaining was frequently observed in the stratum basale (11 out of 16 animals), particularly at the basolateral side (Fig. 3B, D21). At D96, stronger signals were found in the cell membranes of the stratum basale (5 out of 6 animals) and sometimes the stratum spinosum (3 out of 6 animals) (Fig. 3C). Statistical analysis again showed highly significant differences across ages ($P < 0.01$, $n = 4$ or 6), with the highest scores at D96 and lowest at D0 ($P < 0.01$, Tukey's HSD; Fig. 3D). In addition, Pearson correlation coefficient analysis showed strong correlations between UT-B scores and (1) papillae length (0.91), (2) papillae width (0.82), and most interestingly, (3) MCT1 scores (0.83).

Finally, to confirm UT-B staining specificity, antibody removal and peptide competition analysis was performed. Sequential incubation with UT-B and secondary antibodies produced strong staining across epithelial layers (Fig. 4A), whereas no signals occurred in the absence of the UT-B antibody (Fig. 4B). Pre-incubation with the UT-B immunizing peptide prevented any

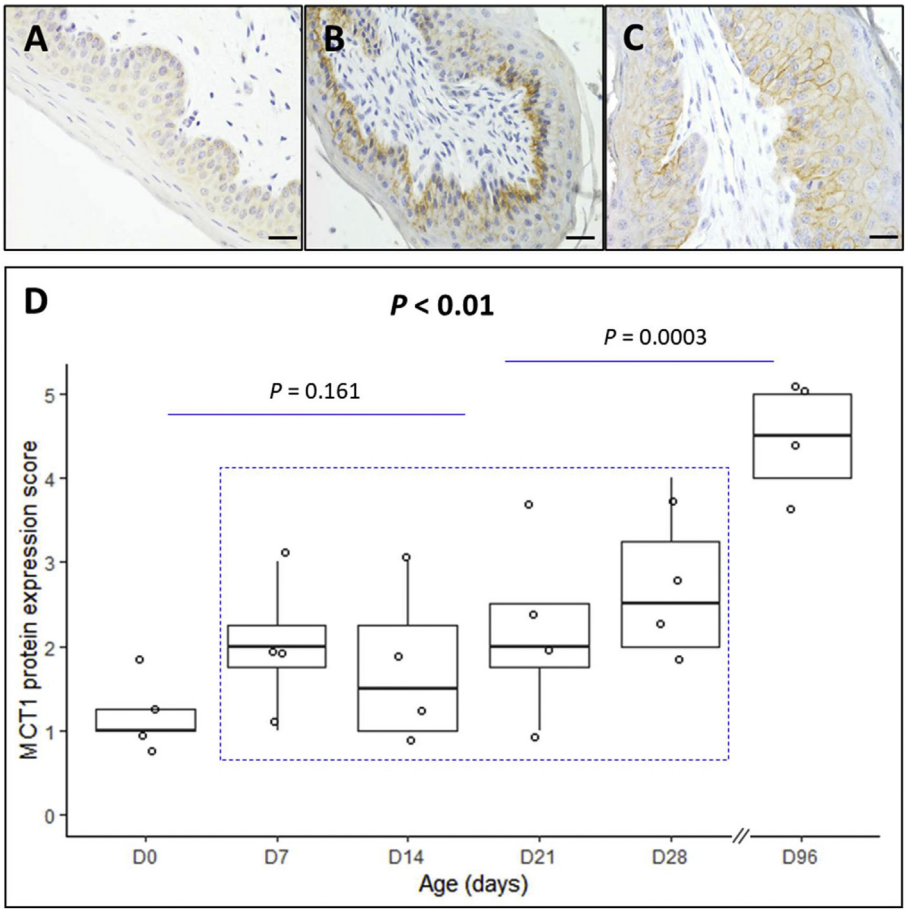

Fig. 2. Ruminal monocarboxylate transporter 1 (MCT1) protein localization and abundance across ages. Representative images showing the staining of MCT1 protein (brown) in the rumen epithelium of calves at birth (A), 28 (B) and 96 d of age (C). The cells were counterstained by haematoxylin to visualize nuclei (dark blue). Scale bar = 25 μm. (D) Signal strength of 4 animals of each age group were blind scored by 3 examiners on a scale of 0 to 5, where 0 = none, 1 = very weak, 2 = weak, 3 = moderate, 4 = strong, 5 = very strong. D0, D7, D14, D21, D28 and D96 represented at birth, 7, 14, 21, 28 and 96 d of age, respectively. Analysis of variance showed statistical difference with ages ($P < 0.01$, $n = 4$).

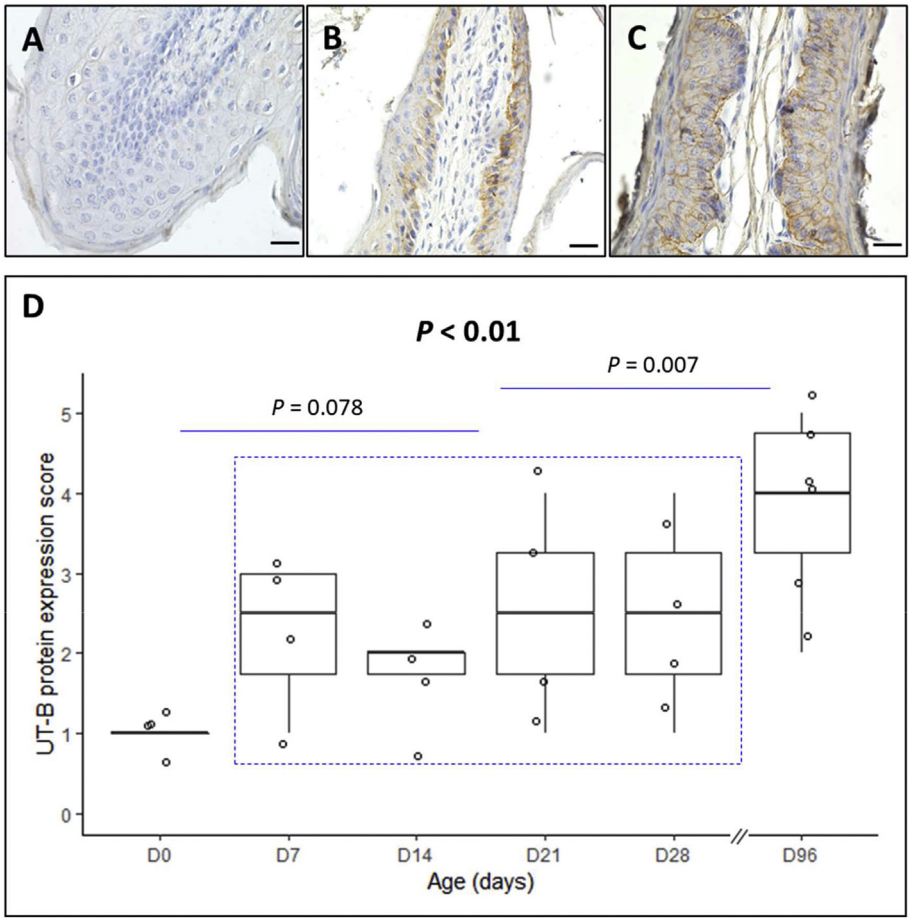

Fig. 3. Ruminal urea transporter B (UT-B) protein localization and abundance across ages. Representative images showing the staining of UT-B protein (brown) in the rumen epithelium of calves at birth (A), 21 (B) and 96 d of age (C). Scale bar = 25 μm. (D) Immunostaining strength of 4 or 6 animals of each age group were blind scored by 3 examiners on a scale of 0 to 5, where 0 = none, 1 = very weak, 2 = weak, 3 = moderate, 4 = strong, 5 = very strong. D0, D7, D14, D21, D28 and D96 represented at birth, 7, 14, 21, 28 and 96 d of age, respectively. Analysis of variance showed significant difference of staining scores across ages ($P < 0.01$, $n = 4$ or 6).

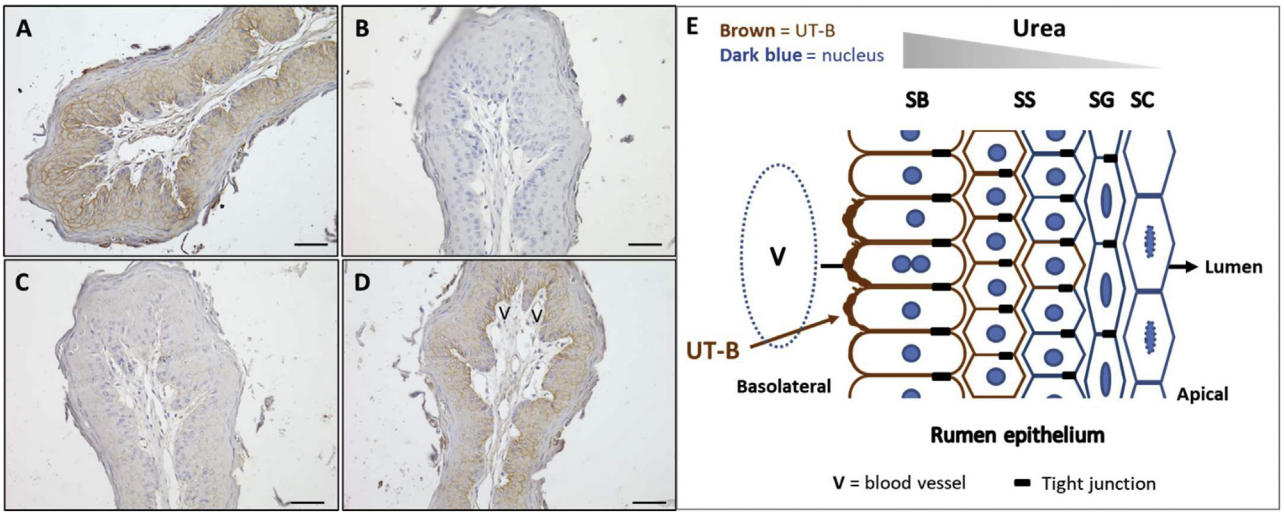

Fig. 4. Primary antibody removal and peptide competition analysis showing the specificity of urea transporter B (UT-B) immunostaining in rumen tissue of calves at 96 d of age. (A) In the presence of the UT-B antibody and a corresponding secondary antibody, strong signals were detected at the stratum basale and the stratum spinosum. (B) In the absence of the UT-B antibody, but presence of the secondary antibody, no signals were generated. (C) Pre-absorption of the UT-B antibody with its specific immunizing peptide prevented most of the signals. (D) In contrast, pre-treatment with a similar amount of non-specific peptide had only a minimal effect on the signals, with the strongest intensity at the basolateral membrane facing blood vessels. Scale bar = 50 μm. (E) Schematic diagram illustrating the general UT-B staining pattern across rumen epithelial layers. SB = stratum basale; SS = stratum spinosum; SG = stratum granulosum; SC = stratum corneum; V = blood vessel.

staining (Fig. 4C), whereas using an equivalent amount of an unrelated peptide had minimal effect (Fig. 4D). Interestingly, UT-B staining was often seen to be strongest in basolateral membranes of the stratum basale cells nearest to blood vessels (Fig. 4D, E).

4. Discussion

Our previous studies have suggested that investigations of ruminal urea transporters should always consider potential alterations at the tissue level (Simmons et al., 2009; Coyle et al., 2016), as well as the cellular level, considering the rumen's highly adaptable morphological response to dietary change. In this current study, we measured the papillae length and width to confirm the basic morphology development of rumen epithelium across ages. In the first month after birth, the rumen epithelium had only slightly developed, potentially initiated by the ad libitum solid feed intake and the resulting fermentation product of SCFA (Flatt et al., 1958; Sander et al., 1959; Tamate et al., 1962). The papillae were short in length and width, with multiple epithelial cells that were small and concisely packed (D14). In contrast, by the third month (D96) the papillae had significantly developed with 4-fold increases in both length and width, due to weaning which occurred at d 56. It should be noted that whilst our simplified procedure to measure papillae was not optimal (cf. measuring dissected papillae), it was sufficient for simply confirming the well-established papillae growth that occurs during rumen development. Although the papillae were still smaller than the measurements commonly reported in adult cows (Coyle et al., 2016), the structure was similar. The epithelial cells had formed the defined shapes of the 4 layers—stratum basale, stratum spinosum, stratum granulosum and stratum corneum (D96)—seen in well-developed rumen epithelia. Denser barrier, balloon cells, and the extensive vascular system (mainly venules with fenestrated endothelium) were also observed.

We next investigated the localization of MCT1 transporters, which transport SCFA across rumen papillae layers and have an expression pattern associated with ruminal microbial fermentation capacity (Flaga et al., 2015). Our data confirmed MCT1 protein predominantly located in the cell membranes of stratum basale and stratum spinosum. The developmental pattern observed was the same as a previous study that comprehensively investigated MCT1 mRNA expression, protein abundance and localization (Flaga et al., 2015)—namely that MCT1 protein increases with age, in association with increased microbially-derived SCFA levels. We suggest that these data validate our use of the blind-scored immunolocalization protocol to semi-quantify the relative levels of ruminal transporter protein.

Our next set of immunolocalization data illustrated where UT-B protein began to develop within the rumen papillae. UT-B protein was frequently observed at the stratum basale cells of the undeveloped papillae and only extended to the stratum spinosum of the more developed papillae. Furthermore, even observed in some of the developed D96 tissues, the most prominent staining was at basolateral membranes of stratum basale cells facing blood vessels—a predicted physiological necessity for moving urea from the blood into the rumen.

Although our UT-B immunolocalization data confirmed an age-dependent change of in situ UT-B protein abundance, the pattern was not a simple linear increase. Instead, it corresponded with the 3 phases of calves' life—namely birth (D0, pre-ruminant), pre-weaning (D7 to D28; transition period) and post-weaning (D96, ruminant). This indicated the apparent stimuli of enhanced UT-B protein abundance to be solid feed intake and weaning. Interestingly, a previous study showed that providing solid feed intake produced a quadratic increase in UT-B mRNA expression—with a dramatic 5-fold increase at the initial provision, then a slight change with the increase of solid feed intake (Berends et al., 2014). This suggested that a change of ruminal local conditions, especially abrupt changes, have dramatic effects on ruminal UT-B mRNA expression. Our findings strongly suggest that similar changes occur with UT-B protein abundance, although perhaps over a more prolonged duration. Finally, it is particularly noteworthy that there was such a strong correlation (0.83) between the immunostaining scores obtained for UT-B and MCT1. This suggests very similar regulatory factors are likely to be involved in controlling the ruminal abundance of these 2 transporters (e.g. SCFA concentration).

It has recently been suggested that microbially-derived SCFA, especially butyrate, might be the direct regulator of rumen urea transport via changing UT-B expression (Lu et al., 2019). SCFA were not measured in this study, but we speculate that the free access to concentrate diet from D7 to D28 enhanced microbial fermentation activity and could explain the initial increase of UT-B protein abundance. As the calves still rely on milk replacer at these stages, rumen function had not reached full capacity and UT-B protein abundance was moderate. From D56 onwards, calves were weaned and fed on concentrate and hay. By D96, the rumen function was greater, now playing a major role in digestion and hence UT-B protein was required at higher levels. From the findings of this initial study, we now believe extensive future studies are required that 1) involve larger numbers of calves, 2) undertake precise measurements of papillae size, dietary intake and ruminal SCFA concentrations, 3) utilize additional techniques to analyze transporter mRNA expression (i.e. real-time PCR) and protein abundance (i.e. Western blotting), and 4) investigate the potential important effect of biological sex on the regulation of ruminal UT-B transporters.

5. Conclusions

This study has characterized UT-B protein localization and abundance in the developing rumen. The UT-B localization pattern agrees well with a functional role of transporting urea from the blood to the rumen, with the age-dependent increases in protein abundance supporting the idea that UT-B regulation occurs directly in response to levels of ruminal SCFA. These findings therefore appear to confirm UT-B involvement in the functioning of the developing bovine rumen.

Author contributions

Chongliang Zhong: conceptualization, formal analysis, investigation, funding, writing – original draft preparation. **Tamsin Lyons**: investigation, writing – original draft. **Orla Heussaff**: validation, investigation. **Evelyn Doyle**: methodology, writing – review and editing, funding. **Eoin O'Hara**: methodology, writing – review and editing. **Sinead Waters**: methodology, writing – review and editing, funding. **David Kenny**: methodology, writing – review and editing, funding. **Gavin Stewart**: conceptualization, writing – original draft preparation, supervision, funding.

Declaration of competing interest

We declare that we have no financial and personal relationships with other people or organizations that can inappropriately influence our work, and there is no professional or other personal interest of any nature or kind in any product, service and/or company that could be construed as influencing the content of this paper.

Acknowledgements

The authors would like to thank Dr. Carl Ng, Ms. Frances Downey, Dr. Carlotta Sacchi and Dr. Alan Farrell for their technical assistance throughout this study. The authors are also grateful to the scholarship funding (CZ) from The China Scholarship Council and University College Dublin.

References

Abdoun K, Stumpff F, Rabbani I, Martens H. Modulation of urea transport across sheep rumen epithelium in vitro by SCFA and CO_2. Am J Physiol Gastrointest Liver Physiol 2010;298:G190–202.

Berends H, van den Borne JJGC, Røjen BA, van Baal J, Gerrits WJJ. Urea recycling contributes to nitrogen retention in calves fed milk replacer and low-Protein solid feed. J Nutr 2014;144:1043–9.

Coyle J, McDaid S, Walpole C, Stewart GS. UT-B Urea transporter localization in the bovine gastrointestinal tract. J Membr Biol 2016;249:77–85.

Flaga J, Górka P, Zabielski R, Kowalski ZM. Differences in monocarboxylic acid transporter type 1 expression in rumen epithelium of newborn calves due to age and milk or milk replacer feeding. J Anim Physiol Anim Nutr 2015;99:521–30.

Flatt WP, Warner RG, Loosli JK. Influence of purified materials on the development of the ruminant stomach. J Dairy Sci 1958;41:1593–600.

Holmes AJ, Chew YV, Colakoglu F, Cliff JB, Klaassens E, Read MN, Solon-Biet SM, McMahon AC, Cogger VC, Ruohonen K, Raubenheimer D, Le Couteur DG, Simpson SJ. Diet-microbiome interactions in health are controlled by intestinal nitrogen source constraints. Cell Metab 2017;25:140–51.

Kristensen NB, Storm AC, Larsen M. Effect of dietary nitrogen content and intravenous urea infusion on ruminal and portal-drained visceral extraction of arterial urea in lactating Holstein cows. J Dairy Sci 2010;93:2670–83.

Lu Z, Stumpff F, Deiner C, Rosendahl J, Braun H, Abdoun K, Aschenbach JR, Martens H. Modulation of sheep ruminal urea transport by ammonia and pH. Am J Physiol Integr Comp Physiol 2014;307:R558–70.

Lu Z, Gui H, Yao L, Yan L, Martens H, Aschenbach JR, Shen Z. Short-chain fatty acids and acidic pH upregulate UT-B, GPR41, and GPR4 in rumen epithelial cells of goats. Am J Physiol Regul Integr Comp Physiol 2015;308:R283–93.

Lu Z, Shen H, Shen Z. Effects of dietary-SCFA on microbial protein synthesis and urinal urea-N excretion are related to microbiota diversity in rumen. Front Physiol 2019;10:1079.

Ludden PA, Stohrer RM, Austin KJ, Atkinson RL, Belden EL, Harlow HJ. Effect of protein supplementation on expression and distribution of urea transporter-B in lambs fed low-quality forage. J Anim Sci 2009;87:1354–65.

Marini JC, Klein JD, Sands JM, Van Amburgh ME. Effect of nitrogen intake on nitrogen recycling and urea transporter abundance in lambs. J Anim Sci 2004;82:1157–64.

Marini JC, Van Amburgh ME. Nitrogen metabolism and recycling in Holstein heifers. J Anim Sci 2003;81:545–52.

Moraïs S, Mizrahi I. The road not taken: the rumen microbiome, functional groups and community states. Trends Microbiol 2019;27:538–49.

O'Hara E, Kenny DA, McGovern E, Byrne CJ, McCabe MS, Guan LL, Waters SM. Investigating temporal microbial dynamics in the rumen of beef calves raised on two farms during early life. FEMS Microbiol Ecol 2020;96:1–16.

Reese AT, Pereira FC, Schintlmeister A, Berry D, Wagner M, Hale LP, Wu A, Jiang S, Durand HK, Zhou X, Premont RT, Diehl AM, O'Connell TM, Alberts SC, Kartzinel TR, Pringle RM, Dunn RR, Wright JP, David LA. Microbial nitrogen limitation in the mammalian large intestine. Nat Microbiol 2018;3:1441–50.

Sander EG, Warner RG, Harrison HN, Loosli JK. The stimulatory effect of sodium butyrate and sodium propionate on the development of rumen mucosa in the young calf. J Dairy Sci 1959;42:1600–5.

Simmons NL, Chaudhry AS, Graham C, Scriven ES, Thistlethwaite A, Smith CP, Stewart GS. Dietary regulation of ruminal bovine UT-B urea transporter expression and localization. J Anim Sci 2009;87:3288–99.

Stewart GS, Graham C, Cattell S, Smith TPL, Simmons NL, Smith CP. UT-B is expressed in bovine rumen: potential role in ruminal urea transport. Am J Physiol Integr Comp Physiol 2005;289:R605–12.

Stewart GS, Smith CP. Urea nitrogen salvage mechanisms and their relevance to ruminants, non-ruminants and man. Nutr Res Rev 2005;18:49–62.

Stumpff F. A look at the smelly side of physiology: transport of short chain fatty acids. Pflug Arch Eur J Physiol 2018;470:571–98.

Tamate H, McGilliard AD, Jacobson NL, Getty R. Effect of various dietaries on the anatomical development of the stomach in the calf. J Dairy Sci 1962;45:408–20.

Tickle P, Thistlethwaite A, Smith CP, Stewart GS. Novel bUT-B2 urea transporter isoform is constitutively activated. Am J Physiol Integr Comp Physiol 2009;297:R323–9.

Walpole C, Farrell A, McGrane A, Stewart GS. Expression and localization of a UT-B urea transporter in the human bladder. Am J Physiol Ren Physiol 2014;307:F1088–94.

Walpole ME, Schurmann BL, Górka P, Penner GB, Loewen ME, Mutsvangwa T. Serosal-to-mucosal urea flux across the isolated ruminal epithelium is mediated via urea transporter-B and aquaporins when Holstein calves are abruptly changed to a moderately fermentable diet. J Dairy Sci 2015;98:1204–13.

Zhong C, Farrell A, Stewart GS. Localization of aquaporin-3 proteins in the bovine rumen. J Dairy Sci 2020;103:2814–20.